

A PEGylated Fluorescent Turn-On Sensor for Detecting Fluoride Ions in Totally Aqueous Media and Its Imaging in Live Cells

Fangyuan Zheng,^[a] Fang Zeng,^{*[a]} Changmin Yu,^[a] Xianfeng Hou,^[a] and Shuizhu Wu^{*[a, b]}

Abstract: Owing to the considerable significance of fluoride anions for health and environmental issues, it is of great importance to develop methods that can rapidly, sensitively and selectively detect the fluoride anion in aqueous media and biological samples. Herein, we demonstrate a robust fluorescent turn-on sensor for detecting the fluoride ion in a totally aqueous solution. In this study, a biocompatible hydrophilic polymer poly(ethylene glycol) (PEG) is incorporated into the sensing system to ensure water solubility and to enhance biocompatibility. *tert*-Butyldiphenylsilyl (TBDPS) groups were

then covalently introduced onto the fluorescein moiety, which effectively quenched the fluorescence of the sensor. Upon addition of fluoride ion, the selective fluoride-mediated cleavage of the Si–O bond leads to the recovery of the fluorescein moiety, resulting in a dramatic increase in fluorescence intensity under visible light excitation. The sensor is responsive and highly selective for the fluoride anion over other common anions; it also ex-

Keywords: fluorescence • fluorescein probes • fluoride • sensors

hibits a very low detection limit of 19 ppb. In addition, this sensor is operative in some real samples such as running water, urine, and serum and can accurately detect fluoride ions in these samples. The cytotoxicity of the sensor was determined to be Grade I toxicity according to United States Pharmacopoeia and ISO 10993-5, suggesting the very low cytotoxicity of the sensor. Moreover, it was found that the sensor could be readily internalized by both HeLa and L929 cells and the sensor could be utilized to track fluoride level changes inside the cells.

Introduction


In recent years, a number of fluorescent sensors for anions have been developed due to fundamental roles of the anions in a wide range of chemical and biological processes.^[1–4] Among these anions, fluoride ions are one of the most attractive targets because of their considerable significance for health and environmental issues.^[5,6] The fluoride ion has unique chemical properties and widely exists in toothpaste and pharmaceutical agents and used for prevention of dental caries, enamel demineralization while wearing orthodontic appliances, and treatment for osteoporosis.^[7] However, a high intake of fluoride can result in serious side effect of fluoride, namely fluorosis, which may cause nephrotoxic changes in both humans and animals and lead to urolithiasis. Fluoride toxicity is also related to an increase in bone densi-

ty or even cancer.^[8] In addition, NaF functions as a potent G-protein activator and Ser/Thr phosphatase inhibitor, and affects plenty of essential cell-signaling elements.^[9] The United States Environmental Protection Agency (EPA) gives an enforceable drinking water standard for fluoride of 4 mg L^{−1} to prevent osteofluorosis and a secondary fluoride standard of 2 mg L^{−1} to protect against dental fluorosis.^[10] The fluoride concentration in urine is commonly used for monitoring fluoride exposure or poisoning.^[11] Therefore, it is of great significance to develop methods that can rapidly, sensitively, and selectively detect the fluoride anion in aqueous media and in such biological samples as urine and serum, as well as inside live cells in terms of human health and environment protection.

Fluorescent chemosensors or probes with high specificity, sensitivity, and ease of operation have received increasing interest;^[12–17] some fluorescent sensors have been reported that are capable of detecting fluoride ions.^[5b, 18–26] The commonly adopted sensing strategy involves supramolecular interactions such as anion- π interactions, hydrogen bonding and Lewis acid/base interactions.^[5b, 18–21] However, most of these sensors are operative only in organic solvents to detect tetrabutylammonium (TBA⁺) fluoride rather than inorganic fluoride salts,^[1, 2a, 5b, 18, 19, 20a, 21] because water would compete significantly with the probe for the anion.^[21b] Moreover, in some cases, the selective recognition of fluoride over oxygen-containing anions (e.g., H₂PO₄[−], CH₃CO₂[−], CO₃^{2−}, and PO₄^{3−}) is restricted.^[21b, 22] On the other hand, another strategy based on the chemical affinity between fluo-

[a] F. Zheng, Prof. F. Zeng, C. Yu, X. Hou, Prof. S. Wu
College of Materials Science & Engineering
South China University of Technology
Guangzhou 510640 (P.R. China)
E-mail: mcfzeng@scut.edu.cn

[b] Prof. S. Wu
State Key Laboratory of Luminescent Materials & Devices
South China University of Technology
Guangzhou 510640 (P.R. China)
Fax: (+86) 20-22236363
E-mail: shzhwu@scut.edu.cn

 Supporting information for this article is available on the WWW under <http://dx.doi.org/10.1002/chem.201202732>.

ride and silicon (fluoride-mediated cleavage of Si–O bond) was developed; *tert*-butyldimethylsilyl (TBDMS) or *tert*-butyldiphenylsilyl (TBDPS) were chosen as additional substituents for the probe molecule, so as to render the probe molecule unreactive to potentially interfering compounds and thus only sensitive to fluoride ions.^[23–26] This approach was first reported by Kim and Swager, who developed a fluorescent fluoride probe in organic solvents, in which the fluorescent response was greatly amplified by using organic semiconducting polymers.^[23a] Subsequently, a couple of studies reported different chemosensors or probes that can detect NaF in aqueous media.^[24–26] For example, Park et al ingeniously developed a 7-hydroxycoumarin-based fluoride sensor containing a *tert*-butyldimethylsilyl (TBDMS) moiety; when excited at 375 nm, this sensor can be used to detect fluoride in water after reaction for 4 h and for imaging of the fluoride anion in living cells.^[26]

Despite these advances in fluorescent fluoride sensors, there is still room for improvement in terms of low detection limit, fast response, as well as usability in totally aqueous solution. In addition, most of the fluoride sensors that are usable in aqueous media require long response times (from several tens of minutes to hours) and UV light excitation, which are not preferable conditions for sensing fluoride in biological samples.

Herein, we demonstrate a robust (responsive, highly sensitive, and visible light-excited) fluorescent sensor for fluoride ion detection in totally aqueous solution and for fluoride imaging in living cells. To ensure water solubility, cell membrane permeability and low-cytotoxicity for the sensor, a hydrophilic polymer poly(ethylene glycol, PEG), which has long been used for a wide range of biomedical applications because of its biocompatible, non-toxic, non-antigenic and non-immunogenic properties, was conjugated into the system. For this sensing approach, TBDPS groups were introduced onto the fluorescein moiety through the reaction of the hydroxy groups on fluorescein with *tert*-butyldiphenylchlorosilane, which quenched the fluorescence of the sensor; upon addition of fluoride ion, the selective fluoride-mediated cleavage of Si–O bond leads to the recovery of the highly fluorescent fluorescein moiety, resulting in a dramatic increase in fluorescence intensity. The schematic illustration for the selective sensing for fluoride anion by the sensor was shown in Figure 1. The sensor based on this PEG-fluorescein-butylidiphenylsilyl architecture demon-

strates several beneficial advantages: First, the preparation of the sensor is technically simple, and it can be easily obtained through a synthetic route involving a two-step-reaction. Second, the PEGylated sensor is able to selectively detect fluoride anions in totally aqueous media (100% water) and in some real samples such as running water, urine, and serum. In addition, it is also capable of permeating the cell membrane and realizing fluoride ion imaging in live cells. Third, the sensor exhibits a fast response to the fluoride ions under visible light excitation, and a low detection limit of 19 ppm, which is the lowest among the reported fluorescent fluoride sensors.

Results and Discussion

Synthesis of the sensor: The sensor (PEG-FITC-Si) was synthesized through a two-step reaction. First, an amine-terminated PEG (methoxypolyethylene glycol amine, with the average molecular weight of 2000, the starting material—PEG2000) was treated with fluorescein isothiocyanate to produce an intermediate product (PEG-FITC), and the hydroxyl groups on fluorescein moiety were then reacted with *tert*-butyldiphenylchlorosilane to form the PEGylated sensor. The synthetic route is shown in Scheme 1.

In this study, the intermediate product and the synthesized sensor were characterized by using a matrix-assisted laser desorption ionization-time of flight (MALDI-TOF) mass spectrometry and ¹H NMR spectroscopy (the Supporting Information, Figure S1 and S2). Unlike a small-molecular compound, which has a definite molecular weight, a polymer sample is actually a mixture of polymer chains with different numbers of repeating units. The commercially obtained PEG sample (methoxypolyethylene glycol amine, with a nominal average molecular weight of 2000) is also comprised of a series of polymer chains with different chain lengths. The molecular weight differences between these PEG chains are multiples of 44.05, namely the molecular weight of the repeat unit of oxyethylene, as shown in Figure S2A (the Supporting Information). As expected, the PEG derivatives (PEG-FITC and the sensor) prepared in this study also exhibit multiple peaks in their MS spectra, as shown in Figure S2 (the Supporting Information). For example, for the starting materials PEG2000 as shown in Figure S2A, the signal centering around *m/z* 1814.8 corre-

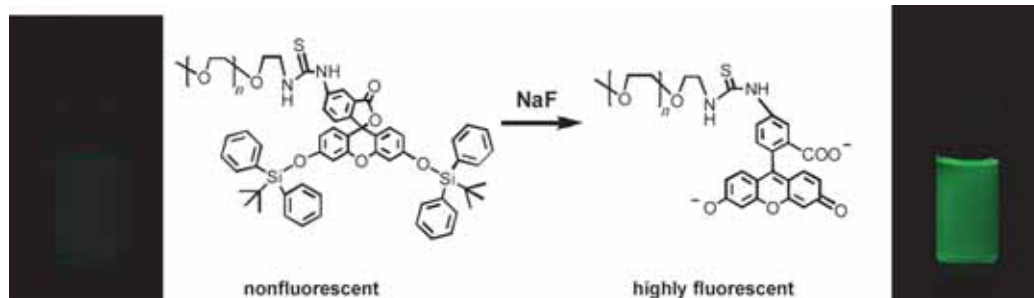
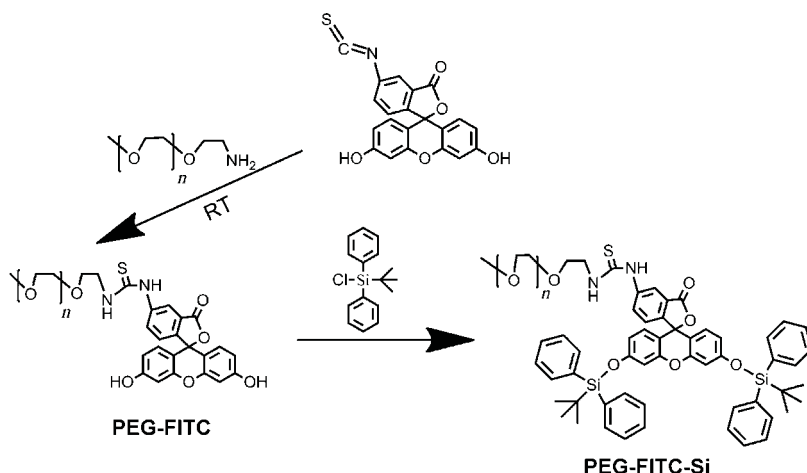


Figure 1. Schematic illustration for the structure of the sensor (PEG-FITC-Si) and its selective detection of fluoride anion (the sensor: 0.2 mg mL⁻¹ in pH 7.4 HEPES buffered water, fluoride anion: 1 × 10⁻⁴ M).



Scheme 1. Synthetic route for the sensor (PEG-FITC-Si).

sponds to the methoxypolyethylene glycol amine with 39 repeat units, and the signal centering around m/z 2204.0 corresponds to PEG-FITC with 39 repeat units (the Supporting Information, Figure S2B), whereas the signal centering around m/z 2681.3 corresponds to the sensor PEG-FITC-Si with 39 repeat units (the Supporting Information, Figure S2C). The detailed assignment and analysis of the mass spectra for the starting material PEG2000, the intermediate product PEG-FITC and the sensor (PEG-FITC-Si) are listed in Table S1 in Supporting Information. On the other hand, it can be seen that in ^1H NMR spectra (the Supporting Information, Figure S1), the backbone protons of the PEG appear at the chemical shifts around $\delta = 3.64$ ppm, and the protons of fluorescein moiety appear at $\delta = 6.2\text{--}7.2$ ppm, whereas the methyl protons of the *tert*-butyldiphenylsilyl groups give rise to peaks at around $\delta = 1.1$ ppm, and the phenyl protons of the *tert*-butyldiphenylsilyl groups give rise to peaks at chemical shifts $\delta = 7.4\text{--}7.9$ ppm. Taken together, the results confirm the successful synthesis of the sensor.

Fluorescent turn-on sensing for F^- in totally aqueous media

(100 % water): The fluorescence spectra of the sensor in aqueous solution upon addition of varied amounts of fluoride anions were shown in Figure 2A. A working curve was also established by plotting the increment of emission intensities at 526 nm versus fluoride anion concentration, as shown in Figure 2B. It is clear that the sensor exhibits very weak emission in the absence of fluoride anion; however, with the addition of the fluoride anion, the fluorescence emission of the sensor gradually increases, and the fluorescence intensity levels off when the concentration of fluoride anion reaches 200 μM . This significant fluorescence amplification can also be observed visually by the fluorescence change as displayed in Figure 1. Moreover, the detection limit was determined as 19 ppb (the Supporting Information, Figure S3), which is, to the best of our knowledge, the lowest among the reported fluorescent fluoride sensors.

We used MALDI-TOF mass spectrometry to investigate the reaction of the sensor with the fluoride anion. A solu-

tion of NaF ($1 \times 10^{-3} \text{ M}$) was added under stirring into the sensor solution (0.2 mg mL^{-1}) in pH 7.4 HEPES-buffered water. Ten minutes later the water was evaporated under vacuum, and the solid residue (reaction product) was purified and then analyzed by mass spectrometry. The MALDI-TOF MS spectra for both the sensor and the product are given in Figure 3. The spectra exhibit multiple peaks because the starting material PEG2000 comprises polymer chains with different lengths, and herein we use one set of MS peaks as

an example to analyze the reaction: In panel A of Figure 3, the signal at around m/z 2637.2 corresponds to a polymer chain of the sensor (PEG-FITC-Si) with 38 repeat units (see the Supporting Information, Table S1); whereas the signal at around m/z 2159.9 in panel B corresponds to a polymer chain of the product whose molecular weight equals that of a PEG-FITC chain with 38 repeat units, and the molecular

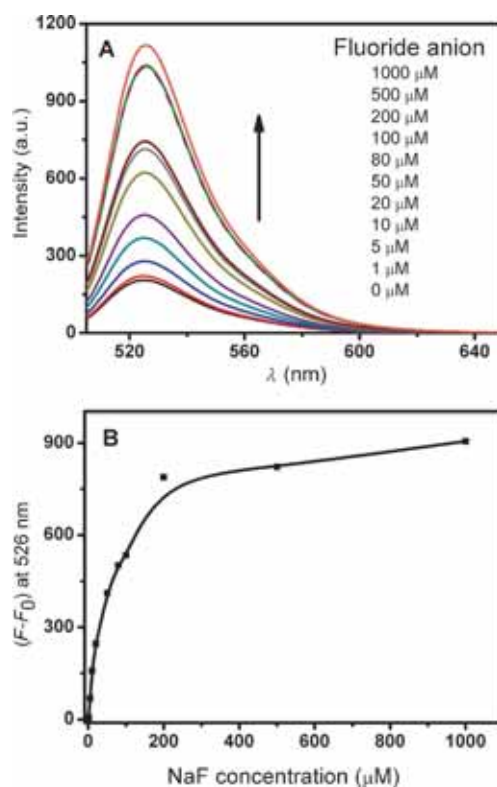


Figure 2. A) Fluorescence spectra of the sensor (0.2 mg mL^{-1}) in the presence of different amounts of F^- in pH 7.4 HEPES buffered water. B) Fluorescence intensity increment ($F - F_0$) of the sensor (0.2 mg mL^{-1}) at 526 nm in the presence of different amounts of F^- in pH 7.4 HEPES buffered water ($\lambda_{\text{ex}} = 490 \text{ nm}$). The spectra were recorded 10 min after addition of fluoride ions.

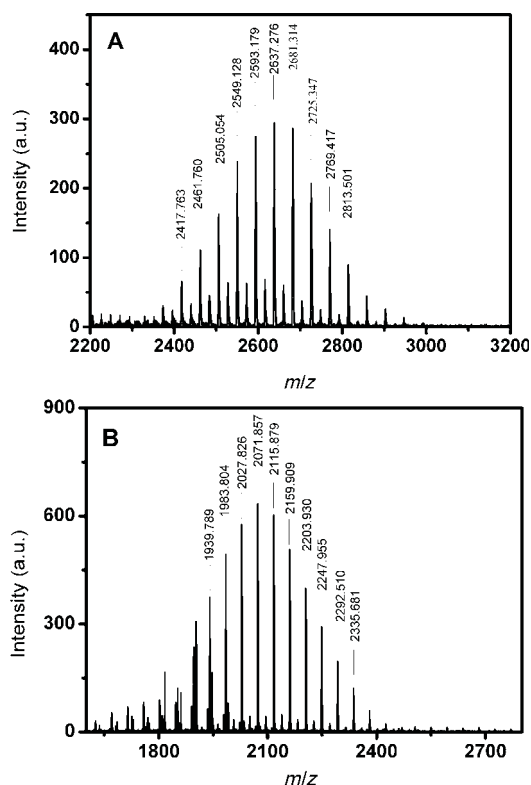


Figure 3. Mass spectra of the as-prepared sensor (A) and the purified reaction product upon addition of fluoride (B).

weight difference (≈ 477) between the product and the corresponding sensor equals the molecular weight of two *tert*-butyldiphenylsilyl groups. This analysis strongly suggests that upon addition of NaF, the two *tert*-butyldiphenylsilyl groups were cleaved from the sensor and the fluorescein moiety was restored. The detailed assignments and analysis for the MS peaks are given in Table S2 (the Supporting Information). For this sensing strategy, in the absence of the fluoride anion, the incorporation of *tert*-butyldiphenylsilyl groups result in the quenching of fluorescence of the sensor; whereas in the presence of fluoride anion, the cleavage of *tert*-butyldiphenylsilyl will restore the fluorescein moiety, thereby leading to the fluorescence enhancement of the sensor.

To further investigate the reaction between the sensor and fluoride ion, first the sensor (PEG-FITC-Si) was allowed to react with NaF in water, and part of the resultant solution was dried and directly used for ^1H NMR measurement; another part of the resultant solution was dried and redissolved in CH_2Cl_2 , and precipitated with diethyl ether several times to remove the cleaved *tert*-butyldiphenylsilyl groups, and the purified chemical also underwent ^1H NMR measurement. These two ^1H NMR spectra were shown in Figure S4 (the Supporting Information). It can be seen from Figure S4B that, for the purified sample, the signals of protons in *tert*-butyldiphenylsilyl groups disappeared, indicating that these groups were cleaved from the sensor molecules. Moreover, by comparing the two spectra in Figure S4 (the

Supporting Information) with those of PEG-FITC and the sensor (Figure S1, the Supporting Information), the spectrum in Figure S4B is very similar to the one in Figure S1A, suggesting the addition of fluoride leads to the restoration of the fluorescein moieties. Based on the ^1H NMR spectra and mass spectra, we proposed the possible mechanism and the reaction equation as shown in the Supporting Information, Figure S5.

To investigate the response time of the sensor towards the fluoride anion, we measured the fluorescence intensity variation as a function of time upon addition of fluoride anion, and the result is shown in Figure 4. The fluorescent intensity of the sensor reached its maximum value within ten minutes upon addition of fluoride anion, which indicates that the reaction between the sensor and the fluoride anion is very fast. The above results demonstrate that the sensor is a responsive system with respect to the fluoride anion.

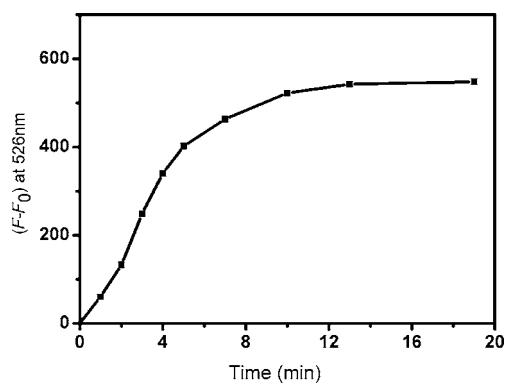


Figure 4. Fluorescence intensity increment ($F - F_0$) at 526 nm of the sensor (0.2 mg mL^{-1}) at different times after addition of F^- ($1 \times 10^{-4} \text{ M}$) in pH 7.4 HEPES buffered water. ($\lambda_{\text{ex}} = 490 \text{ nm}$).

Selectivity and anti-interference performance of the sensing system:

To investigate the selectivity of the sensor towards the fluoride anion over other anions, the fluorescence spectra of the sensor in the presence of other anions including Cl^- , Br^- , I^- , CH_3COO^- , CO_3^{2-} , HCO_3^- , PO_4^{3-} , HPO_4^{2-} , H_2PO_4^- , NO_2^- , NO_3^- , S^{2-} , and SO_4^{2-} were recorded; the comparison of the fluorescence intensities at 526 nm is shown in Figure 5A. It is evident that only F^- induces a prominent intensity enhancement, whereas the addition of other anions under the same conditions led to almost no change in the fluorescence. These results confirm that the sensor shows an excellent selectivity toward F^- over other competitive anions, which is due to the specific reaction of Si-O with F^- . On the other hand, the interference of various anions was also tested. Figure 5B shows the fluorescence response of the sensor towards F^- in the presence of other competitive anions. Evidently, the co-existence of these anions does not interfere with the reaction of fluoride anion with the sensor as well as the subsequent fluorescence enhancement. These results suggest that the probe can function as a highly selective sensor for F^- .

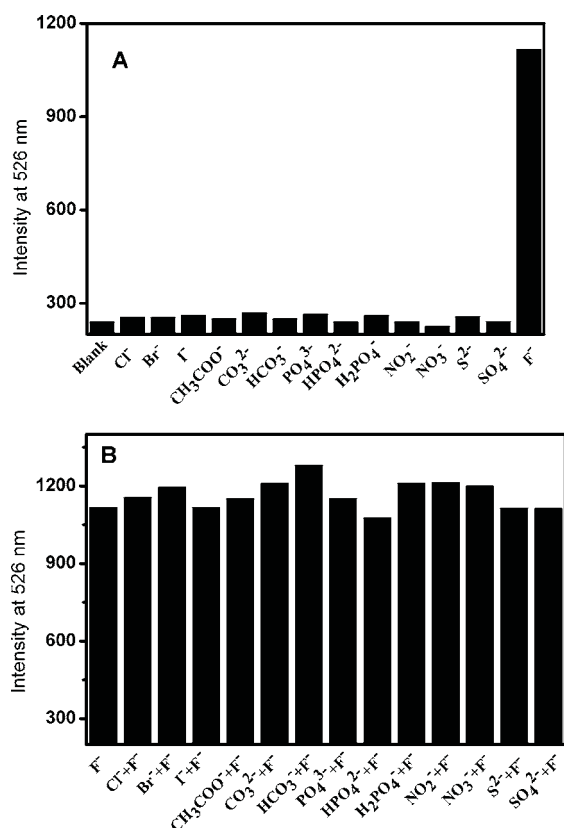


Figure 5. A) Fluorescence intensities at 526 nm for the sensor (0.2 mg mL^{-1}) in the presence of 10^{-3} M different anions. ($\lambda_{\text{ex}}=490 \text{ nm}$). B) Fluorescence intensities at 526 nm for the sensor (0.2 mg mL^{-1}) in the presence of 10^{-3} M of F^{-} and with the addition of 10^{-3} M of different anions respectively. ($\lambda_{\text{ex}}=490 \text{ nm}$). All fluorescence intensities were measured in pH 7.4 HEPES buffered water and 10 min after the addition of anions.

Fluoride ion sensing in running water, human urine, and serum: To evaluate the efficacy of this sensing system in some real samples, the sensor was applied to sensing fluoride ions in samples such as running water, human urine, and fetal bovine serum. As shown in Table 1, this sensor worked quite well in running water, human urine, and serum with the recovery of more than 91%. The results given in Table 1 also show that the detected concentrations of the fluoride anion are in good agreement with those added in real samples. Furthermore, the composition of the running water, urine, and serum do not significantly interfere with the detection of fluoride anion, indicating the potential application of this sensor for the analysis of fluoride anion in real samples. According to EPA, the maximum recommended fluoride concentration in drinking water is 2 mg L^{-1} [10] (about $1 \times 10^{-4} \text{ mol L}^{-1}$); hence, with the detection limit of 19 ppb ($1 \times 10^{-6} \text{ mol L}^{-1}$), this sensor can be used in the detection for fluoride anion in water quality monitoring, as well as in urine and serum samples for diagnosis of fluoride poisoning.

Imaging of the fluoride ion in live cells: To investigate the biocompatibility of the sensor, the cytotoxicity of the sensor

Table 1. Determination of the fluoride anion in running water, human urine, and serum samples.^[a]

Samples	Amount of fluoride [mol L^{-1}]		Recovery [%]
	added	found	
running water	0	—	—
	1.00×10^{-5}	0.93×10^{-5}	93.2
	1.00×10^{-4}	0.95×10^{-4}	94.6
urine	0	—	—
	1.00×10^{-5}	1.04×10^{-5}	104.0
	1.00×10^{-4}	0.99×10^{-4}	98.8
serum	0	—	—
	1.00×10^{-5}	0.92×10^{-5}	91.6
	1.00×10^{-4}	0.92×10^{-4}	92.4

[a] In the test solutions, running water and urine were diluted 10-fold, serum was diluted 100-fold. The measurements were conducted 10 min after the addition of fluoride.

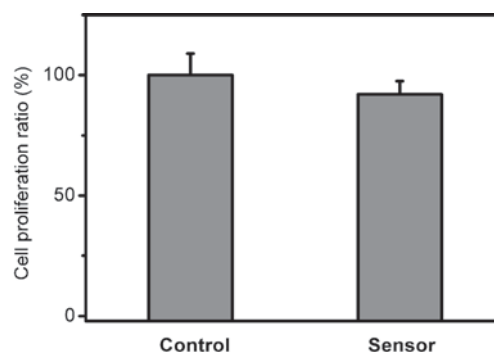


Figure 6. Cytotoxic effects against L929 cells upon 24 h of incubation. Control: L929 cells in the absence of the sensor; sensor: L929 cells in the presence of the sensor at concentration of 0.2 mg mL^{-1} .

was evaluated using L929 cell line by MTT assay in compliance with ISO 10993-5; the results are shown in Figure 6. The sensor shows a cell viability of 92% at the concentration of 0.2 mg mL^{-1} , which belongs to Grade I toxicity according to United States Pharmacopoeia and ISO 10993-5. This indicates that the sensor has very low cytotoxicity.

The favorable features of the sensor include absorption and emission in the visible region, a significant fluorescence turn-on signal, high sensitivity, high selectivity, low cytotoxicity, and efficiency at physiological pH. These desirable characters prompted us to evaluate the ability of the sensor to image F^{-} in living cells. We explored the capability of the sensor to track the fluoride level in two commonly-used cell lines: Hela (human cervical cancer cell) and L929 (murine aneuploid fibrosarcoma cell). Figure 7 displays the fluorescent microscope images for the two kinds of cells incubated with the sensor before and after being treated with fluoride. Probably, due to the PEGylation, the sensor can be easily taken up by both Hela and L929 cells in the RPMI 1640 culture medium; neither the addition of organic solvent (such as DMSO) into the culture medium nor the modification of the sensor (for example, by using acetoxymethyl ester, AM) is needed to enhance the cell membrane permeability of the sensor. Figure 7 also indicates that the internalized sensor compound accumulated in the perinuclear region of the cells.

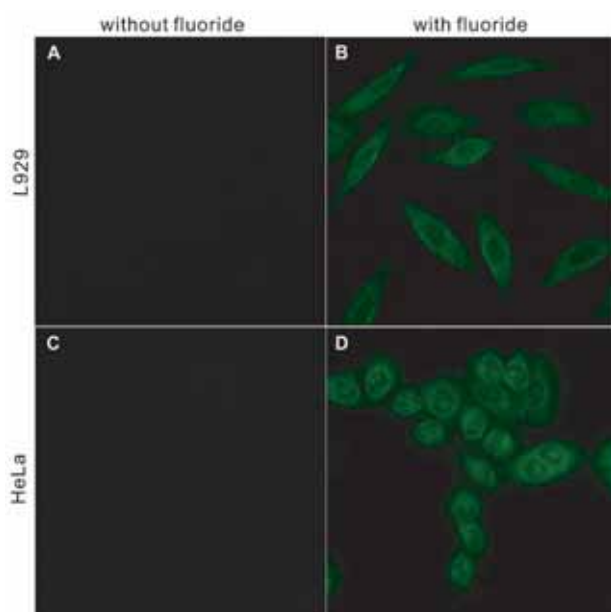


Figure 7. Fluorescence imaging of HeLa and L929 cells incubated with the sensor before (A and C) and after (B and D) being treated with NaF (1×10^{-4} M).

Fluorescence microscope images of both HeLa and L929 live cells loaded with the sensor for 2 h at 37°C show no fluorescence intracellularly, as shown in Figure 7A and C. The control experiment on cells without the sensor gives no fluorescence either under the same exposure condition. In contrast, the intracellular fluorescence for the sensor-stained cells exposed to 1×10^{-4} M of fluoride for 15 min at 37°C gives rise to green fluorescence, as shown in Figure 7B and D. This result indicates that the sensor can be utilized to track fluoride level changes inside living cells.

Conclusion

We have successfully constructed a robust fluorescent turn-on sensing system for use in totally aqueous media, which features a simple synthesis, and the responsive, sensitive, and selective detection of fluoride anions. The PEGylation renders the sensor with good water solubility, cell membrane permeability, as well as very low cytotoxicity. The incorporation of *tert*-butyldiphenylsilyl groups onto fluorescein can effectively quench the fluorescence of the sensor, whereas upon addition of fluoride anions, the fluoride-mediated cleavage of *tert*-butyldiphenylsilyl groups proceeds selectively and quickly, resulting in the recovery of strong fluorescence of fluorescein moiety. This sensor exhibits the lowest limit of detection among those reported fluorescent fluoride sensors. Furthermore, it can be used for detecting fluoride levels in some real samples such as running water, human urine, and serum; it also can be used for imaging fluoride anions inside living cells. Since the sensor is based on an irreversible reaction, this sensor exhibits a low detection limit; however, the disadvantage of this strategy is that the

sensor is not reusable. This sensor might have the potential for application in the detection for fluoride anion in water quality monitoring as well as in diagnosis of fluoride poisoning. This approach offers some useful insights for realizing technically simple fluorescent turn-on sensing in the detection assays for other analytes.

Experimental Section

Materials and reagents: Methoxypolyethylene glycol amine (average molecular weight 2000, PEG2000), fluorescein isothiocyanate, imidazole, *tert*-butyldiphenylchlorosilane, sodium salts of anion (F^- , Cl^- , Br^- , I^- , CH_3COO^- , CO_3^{2-} , HCO_3^- , PO_4^{3-} , HPO_4^{2-} , H_2PO_4^- , NO_2^- , NO_3^- , S^{2-} , SO_4^{2-}), 4-(2-hydroxyethyl)-1-piperazineethanesulfonic acid (HEPES) and *n*-cetyltrimethylammonium bromide (CTAB) were purchased from Aldrich. Human urine was from a healthy male. Fetal bovine serum was supplied by Hangzhou Sijiqing Biological Engineering Materials Co. Ltd. The purified water used in this study was triple-distilled, which was then further treated by ion exchange columns and then by a Milli-Q water purification system. *N,N*-dimethylformamide (DMF) was dried with CaH_2 and vacuum distilled. Methanol and dichloromethane were analytically pure solvents and distilled before use.

Synthesis of the PEG-FITC: Methoxypolyethylene glycol amine (average $M_w=2000$, 0.4 g, 0.2 mmol) and fluorescein isothiocyanate (79 mg, 0.2 mmol) were dissolved in DMF (5 mL) in a flask. The reaction mixture was stirred under N_2 at room temperature overnight; afterwards, the solvent was removed under reduced pressure. The residue was dissolved in CH_2Cl_2 (3 mL), and then diethyl ether (30 mL) was added to precipitate the product. The mixture solution was centrifuged (10000 rev s^{-1} , 8 min). And the product was obtained as a red solid (442 mg, 92%).

Synthesis of the sensor (PEG-FITC-Si): PEG-FITC (430 mg, 0.18 mmol), imidazole (34 mg, 0.5 mmol) were dissolved in CH_2Cl_2 (5 mL) in a flask, the mixture was stirred and cooled in an ice-bath under N_2 . Then, *tert*-butyldiphenylchlorosilane (138 mg, 0.5 mmol) dissolved in CH_2Cl_2 (5 mL) was added into the above solution dropwise. After 1 h, the ice bath was removed, and the solution was stirred at room temperature for another 18 h. After that, the solution was filtered and CH_2Cl_2 (30 mL) was added into the filtrate, which was then washed with deionized water. The combined organic phase was dried in anhydrous MgSO_4 . Then the solvent was evaporated under vacuum and the residue was purified by silica-gel column chromatography by using methanol as an eluent. The product was obtained as a yellow solid (252 mg, 48.8%).

Cytotoxicity: The cell line, L929 (murine aneuploid fibro-sarcoma cell) was incubated in RPMI 1640 medium supplemented with 10% fetal bovine serum (FBS) at 37°C with 5% CO_2 . The cytotoxicity of the sensor against L929 cells was assessed by MTT assay according to ISO 10993-5.

Cell incubation and imaging: Two cell lines, HeLa (human cervical cancer cell) and L929 (murine aneuploid fibrosarcoma cell), were incubated in RPMI 1640 medium supplemented with 10% Fetal Bovine Serum (FBS, Invitrogen). One day before imaging, cells were passed and plated on 30 mm glass culture dishes. Before the experiments, cells were washed with RPMI 1640, incubated in RPMI 1640 medium containing the sensor by use of the sensor stock solution (final sensor concentration 0.2 mg mL^{-1}) at 37°C under 5% CO_2 for 2 hours, washed with PBS, and then treated with a drop of 0.4% trypan blue solution to quench the fluorescence of the sensor adsorbed on the outer cell membrane, so that the observed fluorescence emission comes from the intracellular sensor. After that, the cells were washed three times with PBS and then imaged on an Olympus IX71 inverted fluorescence microscope equipped with a DP72 color CCD (blue light excitation).

Experiments to assess fluoride uptake were performed as follows: the cells stained with the sensor were incubated in the HEPES balanced saline with of sodium fluoride (1×10^{-4} M) for 15 min, and washed with HEPES balanced saline for three times prior to cell imaging.

Measurements: ^1H NMR spectra were recorded on a Bruker Avance 400 MHz NMR spectrometer. Fluorescence spectra were recorded on a Hitachi F-4600 fluorescence spectrophotometer. Absorbance measurements were carried out using a Hitachi U-3010 UV/Vis spectrophotometer. MALDI-TOF mass spectra were measured by using UltrafleXtreme MALDI-TOF system.

As for the measurements for the fluorescence intensity as a function of time, the measurements were conducted in the manual mode, namely once the fluoride was added into the sensor solution, the fluorescence intensity was immediately measured for the time 0, afterwards the fluorescence intensity was measured in the manual mode at certain intervals.

The detection measurements were conducted as follows: First, the stock solution of the sensor (3 mg mL^{-1}) was prepared by dissolving PEG-FITC-Si in HEPES buffered water (pH 7.4) with the addition of a small amount of CTAB (0.036 mg mL^{-1}). The stock solution of NaF was prepared by dissolving NaF in HEPES buffered water (pH 7.4). Afterwards, the test solutions were prepared by adding the requisite amounts of stock solutions together, and then diluting with HEPES buffered water (pH 7.4). The solution was stirred for 10 min, then the fluorescence spectra was recorded.

Acknowledgements

We gratefully acknowledge financial support from NSFC (Project No. 21025415, 21174040) and the National Key Basic Research Program of China.

- [1] R. M. Duke, E. B. Veale, F. M. Pfeffer, P. E. Kruger, T. Gunnlaugsson, *Chem. Soc. Rev.* **2010**, 39, 3936–3953.
- [2] a) E. Galbraith, T. D. James, *Chem. Soc. Rev.* **2010**, 39, 3831–3842; b) V. Amendola, D. Esteban-Gómez, L. Fabbri, M. Licchelli, *Acc. Chem. Res.* **2006**, 39, 343–353; c) P. A. Gale, *Coord. Chem. Rev.* **2001**, 213, 79–128; d) J. L. Sessler, J. M. Davis, *Acc. Chem. Res.* **2001**, 34, 989–997.
- [3] a) R. Martínez-Máñez, F. Sancenón, *Chem. Rev.* **2003**, 103, 4419–4776; b) T. Gunnlaugsson, M. Glynn, G. M. Tocci, P. E. Kruger, F. M. Pfeffer, *Coord. Chem. Rev.* **2006**, 250, 3094–3117; c) Z. M. Hudson, S. Wang, *Acc. Chem. Res.* **2009**, 42, 1584–1596.
- [4] a) A. N. Swinburne, M. J. Paterson, A. Beeby, J. W. Steed, *Chem. Eur. J.* **2010**, 16, 2714–2718; b) Z. H. Zeng, A. A. J. Torriero, A. M. Bond, L. Spiccia, *Chem. Eur. J.* **2010**, 16, 9154–9163.
- [5] a) C. R. Wade, A. J. Broomsgrove, S. Aldridge, F. P. Gabbaï, *Chem. Rev.* **2010**, 110, 3958–3984; b) Z. Xu, S. K. Kim, S. J. Han, C. Lee, G. Kociok-Kohn, T. D. James, J. Yoon, *Eur. J. Org. Chem.* **2009**, 3058–3065.
- [6] a) S. T. Lam, N. Zhu, V. W. W. Yam, *Inorg. Chem.* **2009**, 48, 9664–9670; b) A. E. J. Broomsgrove, D. A. Addy, C. Bresner, I. A. Fallis, A. L. Thompson, S. Aldridge, *Chem. Eur. J.* **2008**, 14, 7525–7529; c) R. Perry-Feigenbaum, E. Sella, D. Shabat, *Chem. Eur. J.* **2011**, 17, 12123–12128.
- [7] a) H. S. Horowitz, *J. Public Health Dent.* **2003**, 63, 3–8; b) J. R. Farley, J. E. Wergedal, D. J. Baylink, *Science* **1983**, 222, 330–332; c) M. Kleerekoper, *Endocrinol. Metab. Clin. North Am.* **1998**, 27, 441–452.
- [8] a) A. Wiseman, *Handbook of Experimental Pharmacology XX/2, Part 2*, 1970, Springer, Berlin, pp. 48–97; b) R. H. Dreisbach, *Handbook of Poisoning*, 1980, Lange Medical Publishers, Los Altos, CA; c) R. E. Gosselin, R. P. Smith, H. C. Hodge, *Clinical toxicology of commercial products*, 1984, Baltimore (MD), Williams & Wilkins; d) B. D. Gessner, M. Beller, J. P. Middaugh, G. M. Whitford, *N. Engl. J. Med.* **1994**, 330, 95–99.
- [9] T. J. Cheng, T. M. Chen, C. H. Chen, Y. K. Lai, *J. Cell. Biochem.* **1998**, 69, 221–231.
- [10] Water: Basic Information about Regulated Drinking Water Contaminants, United States Environmental Protection Agency (EPA) (<http://water.epa.gov/drink/contaminants/basicinformation/fluoride.cfm/>).
- [11] J. Ekstrand, M. Ehrnebo, *J. Occup. Med.* **1983**, 25, 745–748.
- [12] a) N. L. Rosi, C. A. Mirkin, *Chem. Rev.* **2005**, 105, 1547–1562; b) M. Schäferling, O. S. Wolfbeis, *Chem. Eur. J.* **2007**, 13, 4342–4349; c) M. Frigoli, K. Ouadahi, C. Larpent, *Chem. Eur. J.* **2009**, 15, 8319–8330.
- [13] a) S. Amatori, G. Ambrosi, M. Fanelli, M. Formica, V. Fusi, L. Giorgi, E. Macedi, M. Micheloni, P. Paoli, R. Pontellini, P. Rossi, M. A. Varrese, *Chem. Eur. J.* **2012**, 18, 4274–4284; b) D. Maity, A. K. Manna, D. Karthigeyan, T. K. Kundu, S. K. Pati, T. Govindaraju, *Chem. Eur. J.* **2011**, 17, 11152–11161; c) Y. Liu, C. Ma, F. Zeng, S. Z. Wu, *Acta Polym. Sin.* **2012**, 6, 666–672.
- [14] a) T. I. Kim, J. Park, Y. Kim, *Chem. Eur. J.* **2011**, 17, 11978–11982; b) H. S. Peng, J. A. Stolwijk, L. N. Sun, J. Wegener, O. S. Wolfbeis, *Angew. Chem.* **2010**, 122, 4342–4345; *Angew. Chem. Int. Ed.* **2010**, 49, 4246–4249; c) E. M. Nolan, S. J. Lippard, *Chem. Rev.* **2008**, 108, 3443–3480; d) A. Burns, H. Ow, U. Wiesner, *Chem. Soc. Rev.* **2006**, 35, 1028–1042; e) B. Ma, F. Zeng, F. Zheng, S. Wu, *Chem. Eur. J.* **2011**, 17, 14844–14850.
- [15] a) O. S. Wolfbeis, *J. Mater. Chem.* **2005**, 15, 2657–2669; b) H. N. Kim, M. H. Lee, H. J. Kim, J. S. Kim, J. Yoon, *Chem. Soc. Rev.* **2008**, 37, 1465–1472; c) M. I. J. Stich, L. H. Fischer, O. S. Wolfbeis, *Chem. Soc. Rev.* **2010**, 39, 3102–3114.
- [16] a) P. Bosch, F. Catalina, T. Corrales, C. Peinado, *Chem. Eur. J.* **2005**, 11, 4314–4325; b) J. Chen, F. Zeng, S. Z. Wu, Q. M. Chen, Z. Tong, *Chem. Eur. J.* **2008**, 14, 4851–4860; c) N. Dave, M. Y. Chan, P. J. J. Huang, B. D. Smith, J. W. Liu, *J. Am. Chem. Soc.* **2010**, 132, 12668–12673.
- [17] a) D. E. Achatz, R. J. Meier, L. H. Fischer, O. S. Wolfbeis, *Angew. Chem.* **2011**, 123, 274–277; *Angew. Chem. Int. Ed.* **2011**, 50, 260–263; b) G. Fang, M. Y. Xu, F. Zeng, S. Z. Wu, *Langmuir* **2010**, 26, 17764–17771; c) Z. Q. Guo, W. H. Zhu, M. M. Zhu, X. M. Wu, H. Tian, *Chem. Eur. J.* **2010**, 16, 14424–14432; d) H. N. Kim, Z. Q. Guo, W. H. Zhu, J. Yoon, H. Tian, *Chem. Soc. Rev.* **2011**, 40, 79–93.
- [18] a) Z. Q. Liu, M. Shi, F. Y. Li, Q. Fang, Z. H. Chen, T. Yi, C. H. Huang, *Org. Lett.* **2005**, 7, 5481–5484; b) W. J. Xu, S. J. Liu, X. Y. Zhao, S. Sun, S. Cheng, T. C. Ma, H. B. Sun, Q. Zhao, W. Huang, *Chem. Eur. J.* **2010**, 16, 7125–7133.
- [19] a) X. Y. Liu, D. R. Bai, S. N. Wang, *Angew. Chem.* **2006**, 118, 5601–5604; *Angew. Chem. Int. Ed.* **2006**, 45, 5475–5478; b) C. H. Zhao, E. Sakuda, A. Wakamiya, S. Yamaguchi, *Chem. Eur. J.* **2009**, 15, 10603–10612.
- [20] a) Y. Kubo, T. Ishida, A. Kobayashi, T. D. James, *J. Mater. Chem.* **2005**, 15, 2889–2895; b) Y. Kubo, A. Kobayashi, T. Ishida, Y. Misawa, T. D. James, *Chem. Commun.* **2005**, 2846–2848; c) S. J. M. Koskela, T. M. Fyles, T. D. James, *Chem. Commun.* **2005**, 945–947.
- [21] a) Y. Kubo, M. Yamamoto, M. Ikeda, M. Takeuchi, S. Shinkai, S. Yamaguchi, K. Tamao, *Angew. Chem.* **2003**, 115, 2082–2086; *Angew. Chem. Int. Ed.* **2003**, 42, 2036–2040; b) M. Boiocchi, L. D. Boca, D. E. Gomez, L. Fabbri, M. Licchelli, M. Monzani, *J. Am. Chem. Soc.* **2004**, 126, 16507–16514.
- [22] a) Q. Y. Chen, C. F. Chen, *Tetrahedron Lett.* **2004**, 45, 6493–6496; b) P. Das, M. K. Kesharwani, A. K. Mandal, E. Suresh, B. Ganguly, A. Das, *Org. Biomol. Chem.* **2012**, 10, 2263–2271.
- [23] a) T. H. Kim, T. M. Swager, *Angew. Chem.* **2003**, 115, 4951–4954; *Angew. Chem. Int. Ed.* **2003**, 42, 4803–4806; b) S. Y. Kim, J. I. Hong, *Org. Lett.* **2007**, 9, 3109–3112.
- [24] R. Hu, J. Feng, D. Hu, S. Wang, S. Li, Y. Li, G. Yang, *Angew. Chem.* **2010**, 122, 5035–5038; *Angew. Chem. Int. Ed.* **2010**, 49, 4915–4918.
- [25] a) P. Sokkalingam, C. H. Lee, *J. Org. Chem.* **2011**, 76, 3820–3828; b) X. F. Yang, H. P. Qi, L. P. Wang, Z. Su, G. Wang, *Talanta* **2009**, 80, 92–97.
- [26] S. Y. Kim, J. Park, M. Koh, S. B. Park, J. I. Hong, *Chem. Commun.* **2009**, 4735–4737.

Received: July 30, 2012

Revised: October 30, 2012

Published online: November 29, 2012